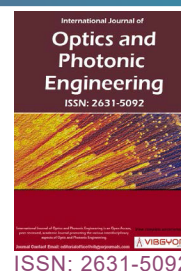


# Pulsed Laser Fragmented Carbon Black Powders for the Synthesis of Carbon Nanodots



**D Reyes<sup>1\*</sup>, M Camacho-López<sup>2\*\*</sup>, L Buendía-González<sup>1</sup>, MA Camacho-López<sup>3</sup>, B Squires<sup>4</sup> and A Neogi<sup>4</sup>**

<sup>1</sup>Facultad de Ciencias, Campus "El Cerrillo", Universidad Autónoma del Estado de México, Toluca, Estado de México, México

<sup>2</sup>Laboratorio de Investigación y Desarrollo de Materiales Avanzados, Facultad de Química, Universidad Autónoma del Estado de México, Campus Rosedal, Km 14.5 Carretera, Toluca Atlacomulco, San Cayetano de Morelos, México

<sup>3</sup>Laboratorio de Fotomedicina, Biofotónica y Espectroscopía Láser de Pulsos Ultracortos, Facultad de Medicina, Universidad Autónoma del Estado de México, Jesús Carranza y Paseo Tolloca s/n, Toluca, México

<sup>4</sup>Department of Physics, University of North Texas, Denton, TX, USA

## Abstract

The pulsed laser fragmentation in liquid media of carbon black (CB) powders using picosecond (ps) laser pulses to produce photoluminescent carbon nanodots (CNDs) is reported. A 1064 nm Nd:YAG pulsed laser with a repetition rate of 15 Hz and 30 ps pulse duration was used. The fragmentation of CB agglomerates suspended in acetone, composed of 80 nm particles, was induced under 10, 20 and 30 min of fragmentation time to reach CNDs with 8 nm diameter average. The PL response of the CNDs solutions shown excitation-wavelength dependence, whose intensity was improved for all the excitation wavelengths with a post-synthesis irradiation by 10 min. The post-irradiation re-fragment the already suspended carbon dots, reaching stable, homogenized and CNDs solutions with similar PL features independently of the F-time. Time-resolved spectroscopy measurements allowed to identify the PL response is characterized by two-lifetime components of 3 ns and 0.15 ns. Raman analysis allowed to observe the D and G peaks characterizing the CNDs and raw material. The CNDs solution showed stable emission and well-dispersion after 9 months. CB is considered a waste material but is shown here as a suitable carbon source to produce CNDs for light emission using the PLFL pathway.

## Keywords

Carbon nanodots, Laser fragmentation, Photoluminescence

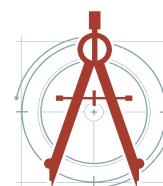
**\*Corresponding author:** D Reyes, Facultad de Ciencias, Campus "El Cerrillo", Universidad Autónoma del Estado de México, Toluca, Estado de México, México;

M Camacho-López, Laboratorio de Investigación y Desarrollo de Materiales Avanzados, Facultad de Química, Universidad Autónoma del Estado de México, Campus Rosedal, Km 14.5 Carretera, Toluca Atlacomulco, San Cayetano de Morelos C.P. 50925, México

**Accepted:** May 05, 2022; **Published:** May 07, 2022

**Copyright:** © 2022 Reyes D, et al. This is an open-access article distributed under the terms of the Creative Commons Attribution License, which permits unrestricted use, distribution, and reproduction in any medium, provided the original author and source are credited.

Reyes et al. *Int J Opt Photonic Eng* 2022, 7:047



**Citation:** Reyes D, Camacho-López M, Buendía-González L, Camacho-López MA, Squires B, et al. (2022) Pulsed Laser Fragmented Carbon Black Powders for the Synthesis of Carbon Nanodots. *Int J Opt Photonic Eng* 7:047

## Introduction

Beside of chemical and biological routes [1,2], the Pulsed Laser Ablation (PLA) is a growing physical route of nanomaterials synthesis, which has shown to be a suitable and green method for the production of carbon-based nanomaterials from both, a solid carbon target, immersed [3,4] or from carbon microparticles suspended [5-7] in a liquid media. In the pulsed laser fragmentation in liquid (PLFL) route, micro or nanoparticles are suspended in a liquid media and then irradiated with laser pulses, which yields, in general, to re-size, re-shape or fragment the suspended material [8,9]. The physical description is based on the fact that in the laser interaction with the suspended material, photodynamic and photothermal effect occurs. Melting and/or vaporization of the suspended particles into atoms or molecules, or the laser-induced Columbic explosion, involving the ejection of photoelectrons or thermal electrons, are the most accepted mechanisms for the production of nanoparticles via PLFL [9]. It is well known in PLFL, several laser parameters (repetition rate, wavelength, pulse energy, pulse duration), solvent (organic, water, mixtures) and suspended material (metallic, oxides, ceramic, and based-carbon) can be tuned to reach nanoparticles with the desired features [10].

Carbon black (CB) is a kind of amorphous carbon that is normally presented as an agglomerate comprising of carbon nanoparticles with different sizes. It has been reported as fill material for the production of conductive polymer composites [11], in electrodes of solar cells [12], for the production of carbon nanostructures [13,14] and among. Concerning the combining of CB and PLFL route for the production of carbon-based nanomaterials it has been not explored at all; laser pulses of 0.4 ms pulse duration and 1064 nm wavelength for the production of nanodiamonds in water from the irradiation during 4 h of CB agglomerates composed of 200 nm particles was reported [13]. Under similar experimental conditions, it was reported the synthesis of hydrophilic carbon onions with hollow cores and incomplete graphitic shells in deionized water from the CB fragmentation under different irradiation times, 1-5 hours [15]. CB suspended (200 nm) in ethanol was fragmented with ms laser pulsed for the production of photoluminescent carbon nanoparticles with amorphous and crystalline structures [16] have been reported.

Using a laser with 0.8 ms pulse duration, the irradiation of CB suspended in Poly (ethylene glycol) (PEG<sub>1500N</sub>) during 2-4 h, the production of both luminescent carbon nanoparticles and carbon nanocages, has been reported [17]. In addition to that, the synthesis of graphitic nanoplatelets and luminescent carbon nanoparticles using 0.3, 0.9, and 1.5 ms laser pulses to fragment graphite flakes in PEG<sub>1500N</sub> solution during 4 h was reported [18]. Using laser pulses of 8 ns pulse duration and 1064 nm wavelength with a per pulse energy 0.7 J with at 10 Hz, the irradiation of CB in ethyl alcohol and aqueous solutions of hexachloroplatinic acid was performed for the formation of rose-like carbon globules containing nanoparticles with a size of 1-5 nm was reported [14]. Graphite powders of 2 µm in average were irradiated with 1064 nm laser pulses while suspended in three kinds of solvents, diamine hydrate, diethanolamine, and PEG<sub>200N</sub> during 2 h to produce carbon nanoparticles of 3.2 and 3.3 nm diameter with functionalized surface [19]. Using ethanol, acetone, or water as solvents, to suspend nano-carbon materials with sizes less than 50 nm, it was reported the successful synthesis of core-shell nanostructures when they were irradiated with a 532 nm pulsed laser (8 ns pulse duration), fixing the repetition rate at 30 Hz. Here, structures where the outer layer was amorphous, and the inner part was onion- or polygon-like carbon with a hollow center were obtained [20].

In this paper, the PLFL of carbon black (CB) powders using ps laser pulses to produce CNDs with PL response is reported. The fragmentation of CB agglomerates suspended in acetone using a 1064 nm Nd:YAG pulsed laser was performed under 10, 20 and 30 min of fragmentation time. The PL response of the CNDs solutions was improved through a post-irradiation after the synthesis by 10 min. Time-resolved spectroscopy allowed to identify the PL response is characterized by two-lifetime components of 3 ns and 0.15 ns. The structural properties of the CNDs were evaluated by Transmission Electron Microscopy (TEM), showing CNDs with 8 nm of diameter on average, while Raman signals confirm the transformation of CB into CNDs structures when observing its intensity.

## Materials and Methods

### Materials and reagents

Carbon black agglomerates composed particles of around 80 nm diameter were purchased by Cabot

Co., CB-Vulcan XC-72. Acetone with 99.9999% pure was achieved by Sigma Aldrich. All materials were used as purchased.

### Laser fragmentation

The laser fragmentation of the carbon black (CB) powders to produce CNDs was carried out with a picosecond (ps) pulsed laser (EKSPLA, Nd:YAG) operating at its fundamental emission of 1064 nm, a repetition rate of 15 Hz and an output beam of 10 mm diameter. The laser source output energy was 30 mJ and 30 ps pulse duration, with an experimental setup as sketched in Figure 1. The sample was prepared with 0.0005 g of CB placed inside a container and then filled with 7 ml of acetone. The laser beam was focused down (using a lens with 130 mm of focal distance) 15 mm above the container's base (30 mm after it reaches the solvent surface), as can be seen in the inset actual picture of Figure 1, such that the laser pulses reaching the CB to induce fragmentation were those after the focal point. The reason to do not place the material to be fragmented in the focal point is to not induce damage on the base of the glass container, which could generate impurities from the glass [10,12]. The spot laser reaching the CB has an area of around 0.08 cm<sup>2</sup>; due to the energy of 30 mJ, it yields to a constant laser fluence of 350 mJ/cm<sup>2</sup>. The obtained solutions were kept at rest by one hour and then carefully taken to another container due to not all the material was fragmented, and it was deposited at the bottom

of the container. The recovered solutions were subject to a post-irradiation process using the same laser irradiation conditions during 10 min. The post-irradiation was performed around 60 min after the synthesis when the solution was changed from container.

### Optical properties characterization

The optical properties of the CNDs solutions were firstly investigated by photoluminescence spectroscopy in a spectrofluorometer (Fluoromax-p). The photoluminescent response of the samples were monitored when these were changed from container and after the post-irradiation processes using 330 nm, 350, 370, 390, 410, and 430 nm excitation wavelengths. Time-resolved PL analysis was performed to obtain lifetimes and characterize the PL response. Those measurements were carried out with a tunable femtosecond Ti:Al<sub>2</sub>O<sub>3</sub> oscillator (Spectra-Physics, Mai Tai, 100 fs, 80 MHz) that was frequency-doubled (tripled) with a BBO crystal via second-harmonic generation. The wavelength of the frequency-doubled beam was varied from 360 to 430 nm, and 300 nm was achieved by frequency tripling. The pump fluence at the sample was kept constant at 6.4 J/cm<sup>2</sup> for all wavelengths. The beam was focused on a quartz cuvette containing the CNDs-based solutions and the emission was collected by fused silica optics. The emission was focused on an imaging spectrometer (Bruker, 250is) equipped with a 150 g/mm grating. The dispersed signal was detected by a streak camera

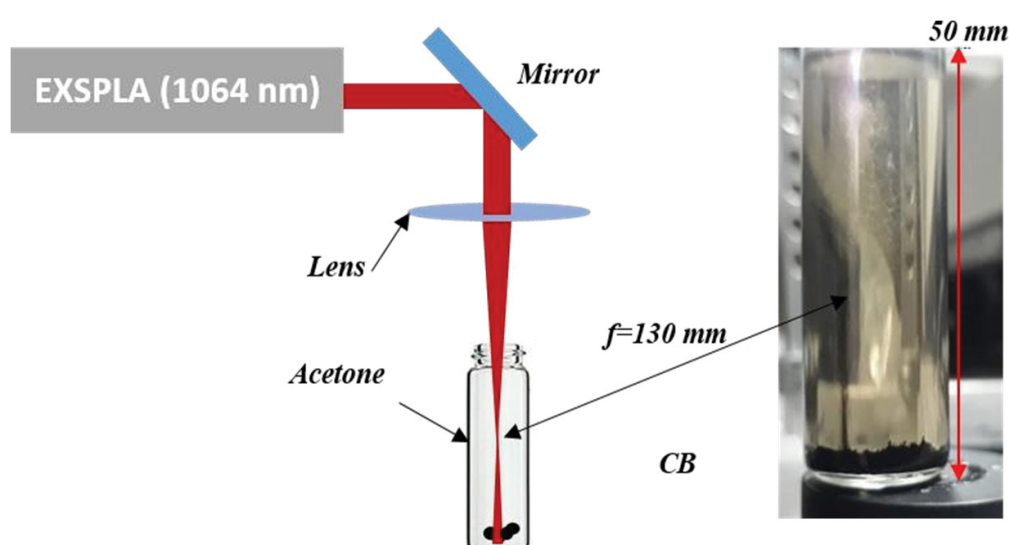


**Figure 1:** Experimental setup for the laser fragmentation process; the inset is an actual picture during the fragmentation.

(Hamamatsu, C4334). Absorption spectroscopy was used to obtain the absorbance features using a double beam spectrometer (Cintra 1010 GBC) in the range 330 - 700 nm only for the samples after the post-irradiation of 10 minutes.

## Structural characterization

The structural characterization of the produced CNDs was performed by Transmission Electron Microscopy (TEM) and Raman spectroscopy only for the sample under 20 min of F-time. Samples for TEM characterization were prepared on Cu grids coated with carbon, by evaporating 3 drops of the colloidal solution on the grid. The TEM and HRTEM measurements were both carried out using a JEOL 2010 transmission electron microscope, at an accelerating voltage of 200 kV. Both the carbon black and the CDs (only for the sample under 20 min of F-Time) were characterized by micro-Raman spectroscopy. A micro-Raman (LabRama HR-800 of Jobin-Yvon-Horiba) system equipped with a He-Ne (632.8 nm) laser and an optical microscope (Olympus, BX-41), with an objective lens of 50 mm was used to focus down the laser beam was used.

## Results and Discussion

### Photoluminescence response

The PL response analysis of the CNDs-based solutions, as was above mentioned, was recorded after these were taken to another container (around 60 min from its synthesis) and after the post-irradiation by 10 minutes. The behavior of the PL response was considerably modified and the intensity enhanced after the post-irradiation. The PL results prior to the post-irradiation are [Figure 2a](#), [Figure 2b](#) and [Figure 2c](#) for 10, 20 and 30 min of F-Time for each excitation wavelength; the intensity interval is fixed for each spectrum for comparison. The PL response of the CNDs solutions is characterized by broad spectrums with non-symmetric shape, with an excitation wavelength-dependent emission behavior, being 350 and 370 nm the excitation wavelength maximizing the intensity emission for the CNDs ([Figure 2a](#)). The broad emission band in this kind of CNDs solutions is related to their polydispersity, which allows emitter centers with different quantum confinement as they have different sizes and surficial features [16,21]. For the larger excitations, 410 and 430 nm, the recorded PL spectrums were not well-defined with low intensity. For 20 and 30 min of F-time, as

shows [Figure 2b](#) and [Figure 2c](#), respectively, the PL intensity decrease around the middle with respect to 10 min sample. As the F-time increase the number of produced CNDs is also increased, yielding to higher concentrated solutions. It has been showed that low-concentrated carbon dots solutions have more efficient light emission due to the lack of absorption/scattering of emitted photons [3], which is the reason of the higher PL intensity for the lowest F-time. The slight increase in the intensity for the 30 min sample could be associated with a higher emitter centers concentration, which also competes with absorption/scattering processes.

It has been shown the constant irradiation of already formed nanostructures in solution, can yields to re-fragmentation process, yielding to their resizing or reshaping [5,7]. The PL response after the post-synthesis irradiation by 10 min for each sample is displayed in [Figure 2d](#), [Figure 2e](#) and [Figure 2f](#) for 10, 20 and 30 min of F-times. It is easily observable the difference in the PL intensity and the shape of the spectrums under each excitation wavelength. For 10 and 30 min of F-time, the excitation maximizing the emission is 370 nm, while for 20 min are both, 350 and 370 nm. For the three CNDs-based solutions, the spectrums for each excitation wavelength turned to be well-defined compared to those prior to the post-irradiation. For 20 min of F-time, for example, the PL intensity increases over 180% and 130% for 350 and 370 nm excitation-wavelength.

The PL intensity for each solution was increased due to the post-irradiation and yielded to well-shaped spectrums independently of the analyzed excitation-wavelength. For the optimum excitation wavelengths, 350 and 370 nm, the FWHM was reduced from 122 nm to 104 nm average, and from 124 to 106 average, respectively, for the sample under 10 min of F-Time, with a blue-shifting, as shown in [Table 1](#). After the post-irradiation, the recorded FWHM were reduced to 102 and 104 nm for 20 min for 350 nm excitation-wavelength, while these were reduced 105 and 107 for 370 nm excitation-wavelength. It could be proposed that the post-irradiation allows to reach homogenized CNDs solutions for the three samples under analysis, with nearly-similar polydispersity but slight concentration of each emitter center with different sizes, which yields to similar FWHM but not the same PL intensity. It is convenient to appoint out the performed structural analysis is



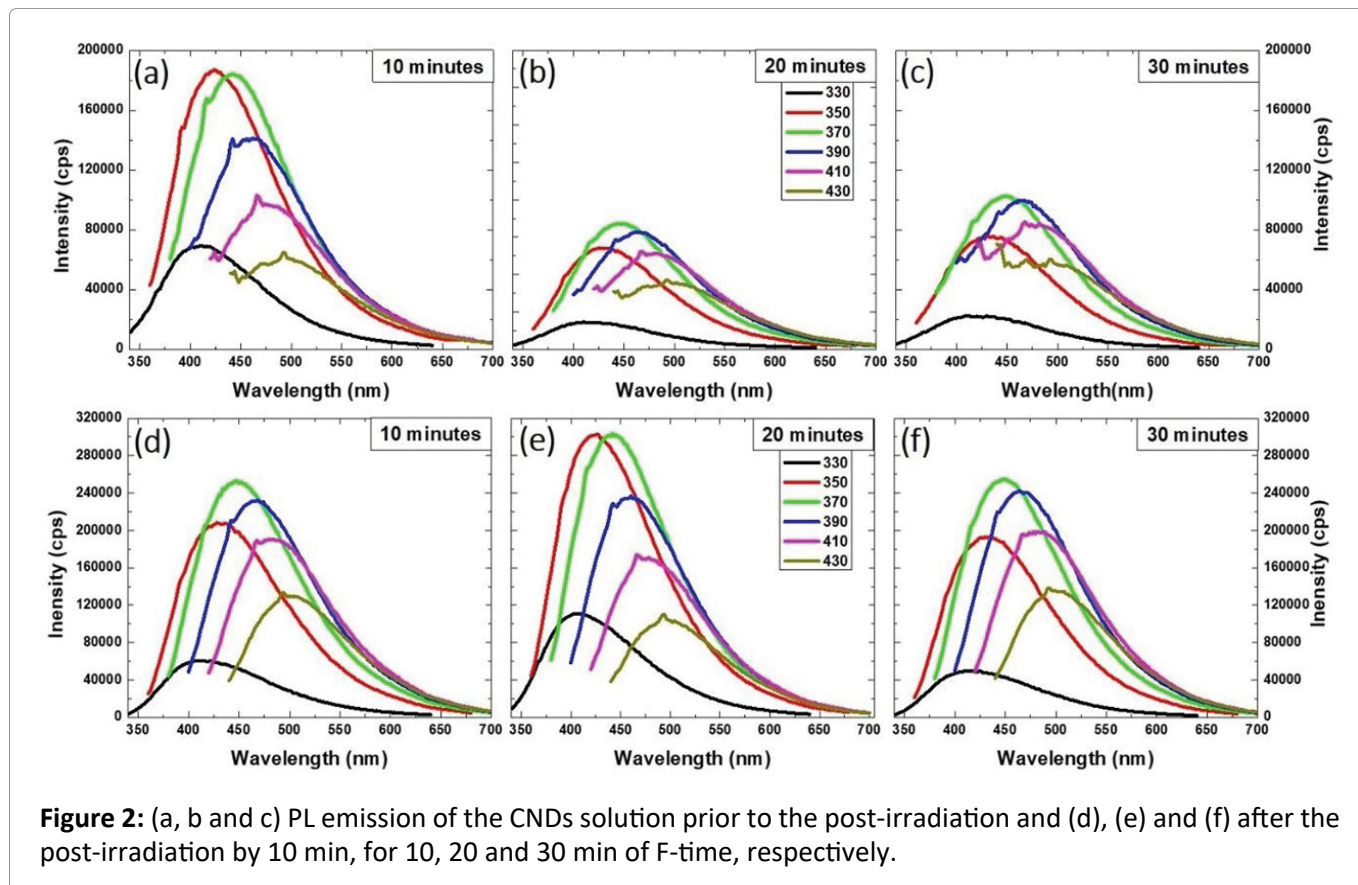


**Figure 2:** (a, b and c) PL emission of the CNDs solution prior to the post-irradiation and (d), (e) and (f) after the post-irradiation by 10 min, for 10, 20 and 30 min of F-time, respectively.

**Table 1:** FWHM and peak position for the three F-times after the synthesis, and after the post- synthesis irradiation by 10 min.

	Excitation wavelength (nm)	10 min	20 min	30 min	10 min	20 min	30 min
		FWHM (nm)			Peak position (nm)		
After the synth	350 nm	122	126	128	412	412	406
<b>10 min of post-</b>		<b>104</b>	<b>102</b>	<b>104</b>	<b>402</b>	<b>402</b>	<b>403</b>
After the synth	370 nm	124	126	124	438	434	440
<b>10 min of post-</b>		<b>106</b>	<b>105</b>	<b>107</b>	<b>421</b>	<b>420</b>	<b>422</b>

not enough to support that asseveration but it is acceptable if consider same emitters will yield to same emission lines.

It has been reported that while emission from excitation below 300 nm is due to excitation of the carbogenic CNDs, the PL response with excitation above 320 nm originates from surface trap states and size-dependence, and it is gradually red-shifted with the increase of the excitation wavelength [22,23], which is the argument supporting the emission observed here. The formation of surface traps is related to the intrinsic process during the laser irradiation, which allows high temperature and ionize the surrounding media; therefore, the

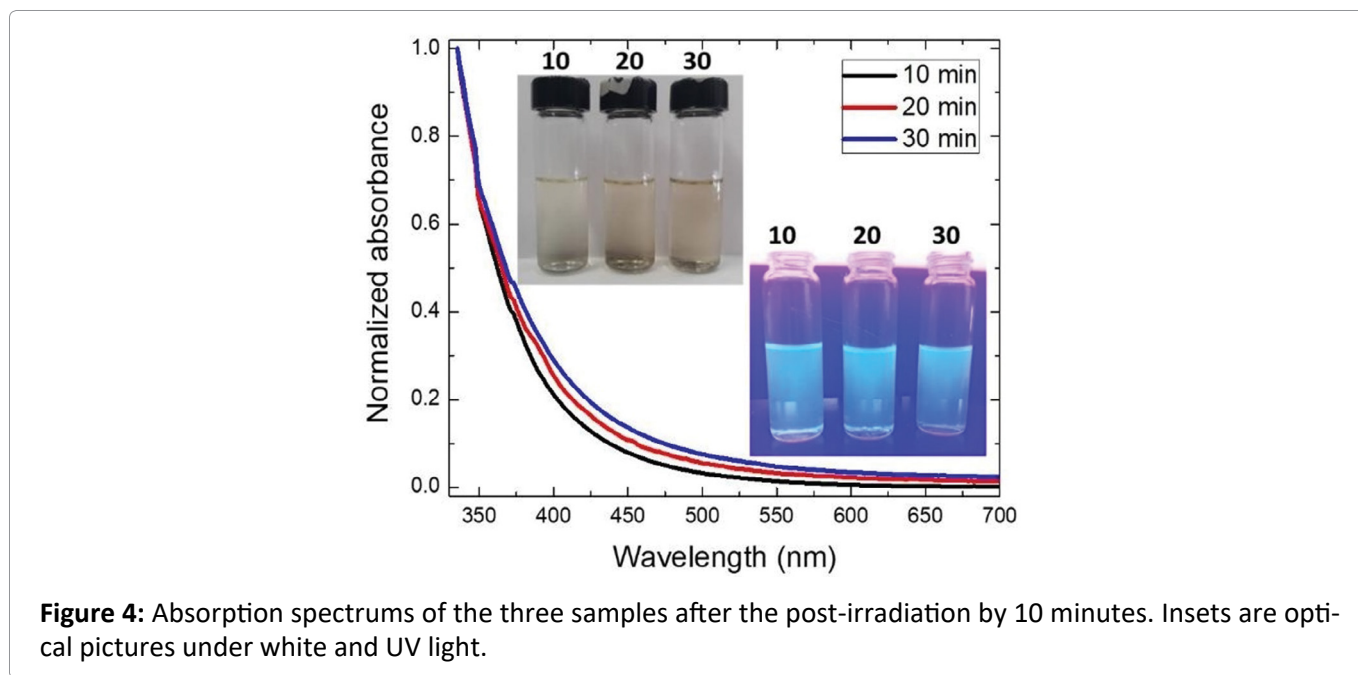
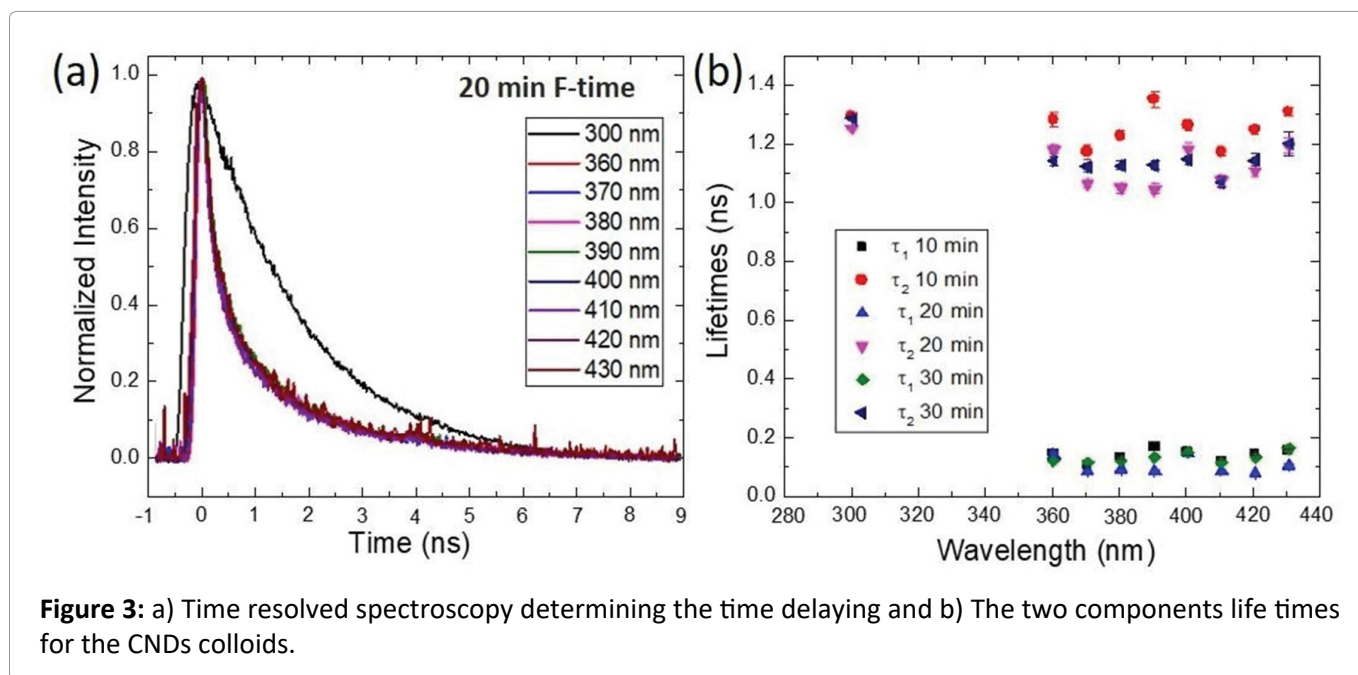
organic molecules possibly graft on the surface of the CNDs, resulting in visible light emission [16,24]. Those surface traps are also inducing passivation effect which helps to stabilize the surface charge of the CNDs to reach stable CNDs solutions [23], 9 months for the solutions reported here. The production of photoluminescent carbon nanostructures using CB and PLFL route has been reported after the irradiation by 2 h of CB suspended in ethanol, but using ms laser pulses at 1064 nm wavelength [16], or after 4 h of irradiation of CB in PEG solution using the same laser [17]. However, the specific effect of the post-synthesis irradiation has been not reported for CNDs solutions. The post-irradiation with 2 MeV protons at different

fluencies, of colloidal core-shell CdSe/ZnS QDs embedded in polyvinyl alcohol (PVOH) induced a PL enhancement for a fluence of  $10^{14}$  H+cm<sup>-2</sup> [25]. The effect on the optical properties of SnS<sub>2</sub> nanoparticles synthesized by liquid phase laser ablation has been also explored [26].

### Time-resolved photoluminescence

The three CNDs solutions were analyzed then with time-resolved PL spectroscopy; results are presented in Figure 3. The typical normalized time-resolved emission is shown in Figure 3a for the sample synthesized by 20 minutes of F-time; for the

other two samples, the spectra look similar and are not included. It can be seen the time decay of the sample when exciting with 360-430 nm wavelength are exciting the same states because the decay shape is virtually identical, although it is broader for 300 nm, indicating the lack of a slow component. Lifetimes were calculated from a biexponential fit of the temporal response, spectrally integrated over the entire emission peak. Figure 3b contains the lifetimes for the three samples for the different excitation wavelengths. The two-lifetime components shown are nearly the same for all the excitations, which suggest the PL response is due



to similar radiative species or CNDs with similar sizes, as was above appointed. From Figure 3b, a lifetime of approximately 1.3 ns ( $1.3 \times 10^{-9}$  s) for the slow component and roughly 0.15 ns ( $0.15 \times 10^{-9}$  s, 150 ps) for the fast component (excitation at 300 nm exhibited no fast component). The origin of the PL response is still unclear until date; the presence of different surface states giving rise to different chromophoric groups is a well-accepted mechanism [27]. Though ultra-fast spectroscopy, it has been reported while the absorption of photons occurs in  $10^{-15}$  s, the radiative emission appears  $10^{-9}$  s [28,29]. According to our time-resolved spectroscopy results, the fast component, 0.15 ns, could be described as a direct transition (singlet), while the slower component, 1.3 ns, could be a non-direct transition (triplet). The Hund's Rule establish the triplet transition has lower energy

than the singlet transition [27,29], which agrees with the recorded PL intensity in Figure 3a.

### Absorption characterization

The absorption properties of the CNDs solutions, were evaluated for the samples only after the post-synthesis irradiation. Figure 4 shows the normalized absorption results for the produced CNDs-based solutions. From Figure 4, the solutions show large absorption for wavelengths below 450 nm which is completely related to the presence of carbon material without peaks giving specific electronic transitions. The largest absorption was found for the sample synthesized with 30 min of F-time, which is due to the presence of a large number of CNDs. The top inset is an actual picture of the solutions from which the typical brown color for this kind of solutions can be observed when

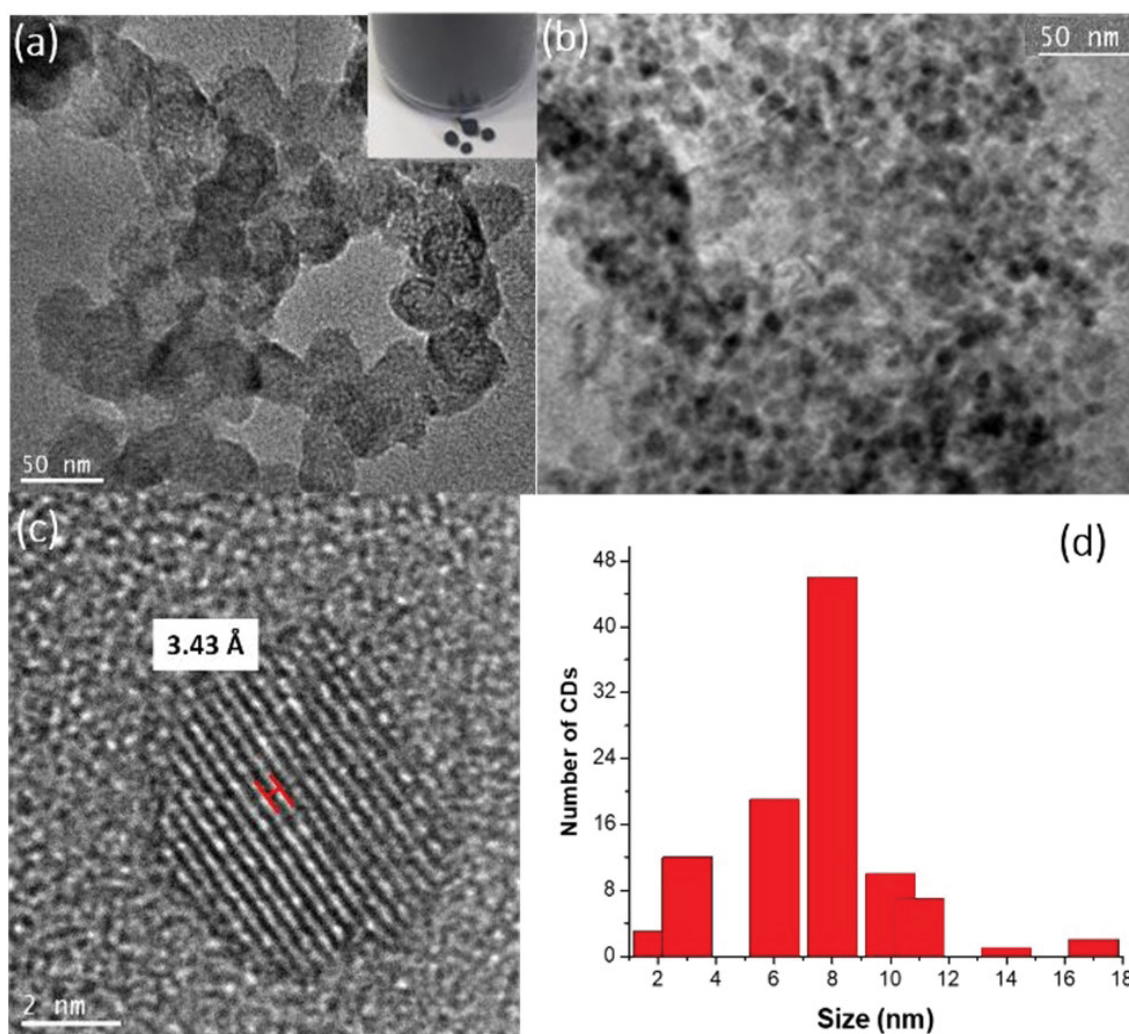


**Figure 5:** a) TEM pictures for the CB nanostructures. Inset-actual CB agglomerates used as raw material; b) TEM results for the produced CNDs, inset is an actual picture; c) HRTEM picture of a CND with 8 nm diameter with a lattice parameter of 3.39 Å. d) Histogram showing the 8 nm average diameter.



illuminated with white light, while the bottom is when they are under a UV lamp emitting at 369 nm, from which a blue-green emission is captured. The green photoluminescence should arise from a state like a band edge state or trap surface states in the carbon dots and is mainly the typical emission color for CNDs solutions [3,21], although red-emissive carbon dots has been also reported [16].

### Structural analysis

To verify the formation of CNDs during the fragmentation process, the corresponding TEM analysis was carried out and pictures were obtained. Figure 5 contains the results of the TEM analysis for the CB before the laser fragmentation and for the prepared CNDs under 20 min of fragmentation time and 10 min of post-irradiation; the extra samples were not structurally analysed. Figure 5a is a TEM picture of the carbon black used as raw material, from which, elliptical and spherical structures of sizes above 60 nm size can be appreciated (80 nm for technical specifications). The inset in Figure 5a is an actual picture of the spherical carbon black agglomerates before the fragmentation process, which has around 1 mm in diameter. TEM images revealed the production of near-spherical nanostructures with different sizes, as can be appreciated in Figure 5b.

HRTEM allowed showing the production of CNDs with an average diameter of 8 nm, as can be appreciated in Figure 5c and the histogram showed

in Figure 5d, which was obtained by counting around 140 CNDs. In Figure 5c, the interlayer-spacing of the carbon dots structure was identified as 3.43 Å. It is well accepted that the interlayer-spacing of graphitic carbon decreases as the degree of crystallinity increases [30]. According to the card (PDF Number: 41-1487), the interlayer spacing of 3.3756 Å corresponds to the (002) index [30,31], which is nearly what was found here. This distance indicates the material is merely a graphitic carbon, not crystalline graphite, by virtue of an interlayer spacing of 3.3553 Å is consider for crystalline graphite.

As is evident from Figure 5a and Figure 5c, carbon black spheres, composed of 60 nm nanostructures, were transformed to fewer CNDs with 8 nm of diameter on average. Koshizaki and coworkers reported the production of core-shell structures, with an amorphous layer and an inner part with onion or polygon-like carbon, after laser irradiation (ns, 532 nm) of 50 nm carbon nanoparticles [23]. Here, using ps laser pulses of 1064 nm and CB as raw material, CNDs were produced. The formation of the as obtained CNDs could be described as follows. In the first stage, the energy of the laser pulses is absorbed by the original CB spheres which induce its fragmentation into their nanoscale components, around 60 nm size in the used CB here. In a second stage, the components of the CB interact with consecutive laser pulses and are re-fragmented, induce a size reduction [18,32], leading to more

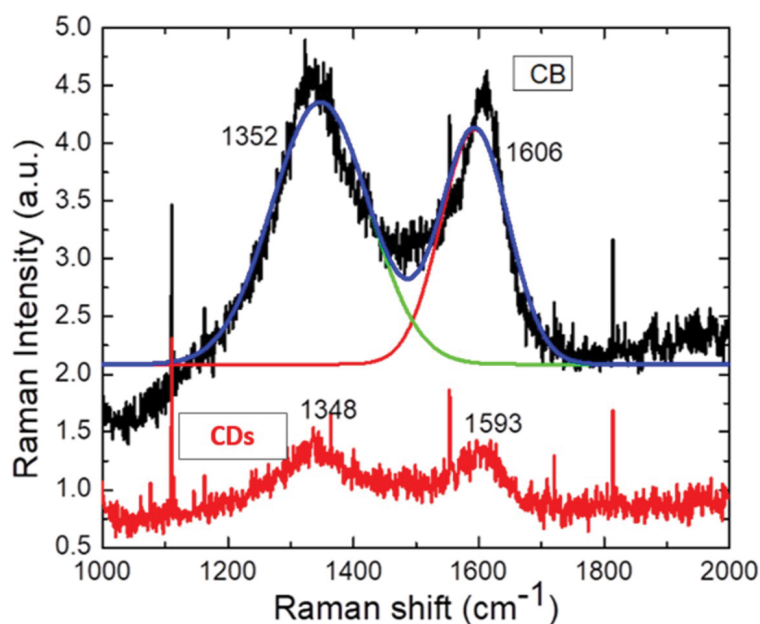


**Figure 6:** Raman signal of the CB raw material and the produced CNDs.



stable CNDs solutions. In a third stage, during the 10 minutes of post-irradiation, the laser pulses still induce a re-fragmentation effect in the suspended CNDs, yielding to a well-dispersed CNDs solution with probably similar particle distribution. The previous appointment matches with near-similar absorption and PL features previously described. Even when a deeper HRTEM analysis for the three samples is missing, due to technical details, the reported optical and structural results for 20 min of F-time sample are consistent.

The Raman analysis of both the CB powders before the laser fragmentation process and the obtained CNDs is displayed in Figure 6, which allowed the identification of the typical Raman peaks characterizing both structures. Raman spectra of the CB show the D band at  $1352\text{ cm}^{-1}$ , which is related to  $\text{sp}^3$ -hybridized carbon atoms in a cubic structure, and G band at  $1606\text{ cm}^{-1}$ , associated with amorphous  $\text{sp}^2$ -bonded forms of carbon. The intensity ratio was calculated as,  $I_D/I_G = 1.013$ , which is theoretically related to a graphitic disorder structure when its value exceeds the unit [30,33]. For CB Vulcan-XC72, D and G peaks have been reported at  $1371$  and  $1604\text{ cm}^{-1}$  [33,34], respectively. D and G Raman peaks for the CNDs were identified at  $1348\text{ cm}^{-1}$  and  $1593\text{ cm}^{-1}$ , respectively (Figure 6, red line), which are agreement with previous reports [9],  $1347.3$  and  $1583.4\text{ cm}^{-1}$  for both bands.

As can be appreciated from Figure 6, the Raman intensity considerably decreases for the CNDs compared with the CB powders; the decrement of the intensity of the Raman signal is attributed to a diminishing of the size particle [35]. As was indicated in the experimental section, the CB powders are agglomerates of around  $60\text{ nm}$  size so; the size reduction to less than  $10\text{ nm}$  ( $8\text{ nm}$  on average) is visible in Figure 5a and Figure 5b, which agrees with the size Raman intensity dependent on the size particle.

## Conclusions

In conclusion, the fragmentation of CB using ps laser pulses for the synthesis of photoluminescent CNDs-based solutions using PLFL method was reported. The PL response after the synthesis and post-irradiation was successfully described. The PL emission was found to be wavelength-dependent and characterized by a broad and Gaussian emission band, which is red-shifted when the excitation

wavelength increases. The post-irradiation showed to be useful to improve the light emission. TEM measurements identified the presence of graphitic CNDs with an average diameter of  $8\text{ nm}$  ( $60\text{ nm}$  for the CB used as raw material). It is convenient to appoint out the combination of PLFL method, CB and picosecond laser pulses has been not explored as using nano or microsecond pulses. Particularly microsecond pulses require over 4 hours of irradiation, while here, results showed the optical properties of CNDs solutions can be optimized with 10 minutes of F-time and 10 minutes of a post-irradiation process. In general, CB is considering a waste material, however, their use as raw material for the production of CNDs is being successfully reported, which is important besides the fact the lack of experimental results related to this topic.

## Acknowledgements

This work was partially supported by NSF sponsored EFRI: NewLAWproject entitled, 'GOALI:EFRI NewLaw: Non-reciprocal effects and Anderson localization of acoustic and elastic waves in periodic structures with broken P-symmetry of the unit cell' Award#1741677.

## References

1. Xia C, Zhu S, Feng T, Yang M, Yang B (2019) Evolution and synthesis of carbon dots: from carbon dots to carbonized polymer dots. *Adv Sci* 6: 1901316.
2. Bhattacharya D, Kumar V, Packirisamy G (2021) Biocompatible carbon nanodots from red onion peels for anti-oxidative and bioimaging applications. *Mater Express* 11: 1958-1965.
3. Reyes D, Camacho M, Camacho M, Mayorga M, Weathers D, et al. (2016) Laser ablated carbon nanodots for light emission. *Nanoscale Res Lett* 11: 424.
4. Małolepszy, Błonski S, Chrzanowska J, Wojasiński M, Płocinski T, et al. (2018) Fluorescent carbon and graphene oxide nanoparticles synthesized by the laser ablation in liquid. *Appl Phys A* 124: 282.
5. Doñate C, Torres R, Pyatenko A, Falomir E, Fernández M, et al. (2018) Fabrication by Laser irradiation in a continuous flow jet of carbon quantum dots for fluorescence imaging. *ACS Omega* 33: 2735-2742.
6. Viguera E, Hernández S, Camacho MA, Reyes D, Farías R, et al. (2016) Optical properties of carbon nanostructures produced by laser irradiation on chemically modified multi-walled carbon nanotubes. *Optics & Laser Technology* 84: 53-58.

7. Zhou J, Booker CJ, Li RL, Zhou X, Sham TK, et al. (2007) An electrochemical avenue to blue luminescent nanocrystals from multiwalled carbon nanotubes (MWCNTs). *J Am Chem Soc* 129: 744-745.
8. Maximova K, Aristov A, Sentis M, Kabashin AV (2015) Size-controllable synthesis of bare gold nanoparticles by femtosecond laser fragmentation in water. *Nanotechnology* 26: 065601.
9. Zeng H, Yang S, Cai W (2011) Reshaping formation and luminescence evolution of ZnO quantum dots by laser-induced fragmentation in liquid. *Phys Chem C* 115: 5038-5043.
10. Zeng H, Du XW, Singh SC, Kulinich SA, Yang S, et al. (2012) Nanomaterials via laser ablation/irradiation in liquid: A review. *Adv Funct Mater* 22: 1333-1353.
11. Hernández S, Viguera E, Mayorga M, Reyes D (2012) Changes in the electrical resistivity of thin-films for polymer composites induced by heating-cooling cycles. *J Mat Sci and Eng B* 2: 601.
12. Huang Z, Liu X, Li K, Li D, Luo Y, et al. (2007) Application of carbon materials as counter electrodes of dye-sensitized solar cells. *Electrochem Comm* 9: 596-598.
13. Hu S, Tian F, Bai P, Cao S, Sun J, et al. (2009) Synthesis and luminescence of nanodiamonds from carbon black. *Materials Science & Engineering B* 157: 11-14.
14. Ivashchenko OV, Trenikhin MV, Kryazhev YG, Tolochko BP, Eliseev VS, et al. (2015) Structural transformations of carbon black by high-energy laser and electron irradiation. *Nanotech in Russia* 10: 696-700.
15. Hu S, Bai P, Tian F, Cao S, Sun J (2009) Hydrophilic carbon onions synthesized by millisecond pulsed laser irradiation. *Carbon* 47: 876-883.
16. Li H, Su D, Gao H, Yan X, Kong D, et al. (2020) Design of red emissive carbon dots: robust performance for analytical applications in pesticide monitoring. *Anal Chem* 92: 3198-3205.
17. Hu S, Dong Y, Yang J, Liu J, Cao S (2012) Simultaneous synthesis of luminescent carbon nanoparticles and carbon nanocages by laser ablation of carbon black suspension and their optical limiting properties. *J Mater Chem* 22: 1957-1961.
18. Hu S, Liu J, Yang J, Wang Y, Cao S (2011) Laser synthesis and size tailor of carbon quantum dots. *J Nanopart Res* 13: 7247-7252.
19. Hu SL, Niu KY, Sun J, Yang J, Zhao NQ, et al. (2009) One-step synthesis of fluorescent carbon nanoparticles by laser irradiation. *J Mater Chem* 19: 484.
20. Li X, Wang H, Shimizu Y, Pyatenko A, Kawaguchi K, et al. (2010) Preparation of carbon quantum dots with tunable photoluminescence by rapid laser passivation in ordinary organic solvents. *Chem Comm* 47: 932-934.
21. Liu Y, Zheng J, Liu W, Yuan Z, Lu C (2022) Steady-state and dynamic bioanalysis using carbon quantum dot-based luminescence probes. *Chem Nano Mat* 8: e202200013.
22. Zeng Z, Zhang W, Arvapalli DM, Bloom B, Sheardy A, et al. (2017) A fluorescence-electrochemical study of carbon nanodots (CNDs) in bio- and photoelectronic application and energy gap investigation. *Phys Chem Chem Phys* 19: 20101-20109.
23. Kwon W, Do S, Kim JH, Jeong MS, Rhee SW (2015) Control of photoluminescence of carbon nanodots via surface functionalization using parasubstituted anilines. *Sci Rep* 5: 12604.
24. Sun YP, Zhou B, Lin Y, Wang W, Fernando KAS, et al. (2006) Quantum-sized carbon dots for bright and colorful photoluminescence. *J Am Chem Soc* 128: 7756-7757.
25. Zanazzi E, Favaro M, Ficorella A, Pancheri L, Dall Betta GF, et al. (2019) Photoluminescence enhancement of colloidal CdSe/ZnS quantum dots embedded in polyvinyl alcohol after 2 MeV proton irradiation: Crucial role of the embedding medium. *Optical Materials* 88: 271-276.
26. Johnny J, Sepulveda S, Krishnan B, Aguilar Martinez JA, Avellaneda Avellaneda D, et al. (2019) SnS<sub>2</sub> nanoparticles by liquid phase laser ablation: Effects of laser fluence, temperature and post irradiation on morphology and hydrogen evolution reaction. *App Surf Sci* 470: 276-288.
27. Khan S, Gupta A, Verma NC, Nandi CK (2015) Time-resolved emission reveals ensemble of emissive states as the origin of multicolor fluorescence in carbon dots. *Nano Letts* 15: 8300-8305.
28. Wang H, Sun C, Chen X, Zhang Y, Colvin VL, et al. (2017) Excitation wavelength independent visible color emission of carbon dots. *Nanoscale* 9: 1909-1915.
29. Valeour B (2001) Molecular fluorescence: Principles and applications. Wiley-VCH, New York.
30. Howe JY, Rawn CJ, Jones LE, Ow H (2003) Improved crystallographic data for graphite. *Powder Diffraction* 18: 150-154.
31. Oberlin A (1989) Chemistry and physics of carbon. In: Walker PJ, Thrower P, Vol. 22, edited by (Dekker, New York.

32. Pyatenko A, Wang H, Koshizaki N, Tsuji T (2013) Mechanism of pulse laser interaction with colloidal nanoparticles. *Laser Photonics Rev* 7: 596-604.
33. Jawhari T, Roid A, Casado J (1995) Raman spectroscopic characterization of some commercially available carbon black materials. *Carbon* 33: 1561-1565.
34. Zhou J, Sheng Z, Han H, Zou M, Li C (2012) Facile synthesis of fluorescent carbon dots using watermelon peel as a carbon source. *Materials Letters* 66: 222-224.
35. Gómez DA, Coello J, Maspoch S (2019) The influence of particle size on the intensity and reproducibility of Raman spectra of compacted samples. *Vibrational Spectroscopy* 100: 48-56.

